

A Segmented Robot Grasping Perception Neural Network for Edge AI

Casper Bröcheler, Thomas Vroom, Derrick Timmermans, Alan van den Akker,

Guangzhi Tang, Charalampos S. Kouzinopoulos, Rico Möckel

Department of Advanced Computing Sciences

Maastricht University

Maastricht, Netherlands

{c.brocheler, t.vroom, dxy.timmermans, alan.vandenakker, guangzhi.tang, charis.kouzinopoulos, rico.mockel}@maastrichtuniversity.nl

Abstract—Robotic grasping, the ability of robots to reliably secure and manipulate objects of varying shapes, sizes and orientations, is a complex task that requires precise perception and control. Deep neural networks have shown remarkable success in grasp synthesis by learning rich and abstract representations of objects. When deployed at the edge, these models can enable low-latency, low-power inference, making real-time grasping feasible in resource-constrained environments. This work implements Heatmap-Guided Grasp Detection, an end-to-end framework for the detection of 6-Dof grasp poses, on the GAP9 RISC-V System-on-Chip. The model is optimised using hardware-aware techniques, including input dimensionality reduction, model partitioning, and quantisation. Experimental evaluation on the GraspNet-1Billion benchmark validates the feasibility of fully on-chip inference, highlighting the potential of low-power MCUs for real-time, autonomous manipulation.

Index Terms—Grasping perception, MCU, GAP9, RISC-V, edge AI, embedded systems

I. INTRODUCTION

Object grasping synthesis is a fundamental challenge in robotics, underpinning applications such as automated warehouse operations, patient assistance in healthcare, and object sorting on assembly lines [1]. While humans excel at grasping objects of various shapes and sizes with precision, replicating this ability in robotics remains challenging. Insufficient grip strength may result in objects slipping, while excessive force risks damaging fragile or valuable items [2].

A recent trend in Deep Learning (DL) research is *Edge AI*, which shifts computation from the cloud to resource-constrained devices at the network’s edge, enabling low-latency inference and re-training on energy-efficient Microcontroller Units (MCUs) [3] [4] [5]. However, deploying DL models on MCUs for real-time robotic grasping presents significant challenges due to strict constraints on memory, processing power, and energy availability. Unlike cloud or high-performance computing paradigms, Edge AI implementations must be highly optimised, balancing model size, execution efficiency, and power consumption, while maintaining high levels of grasping accuracy and robustness.

This work performs robotic grasping inference at the edge. To reduce memory and computational requirements, a series

of hardware-aware optimisation techniques are applied. These include the reduction of the input resolution from the original RGB-Depth (RGBD) data, employing pipelined execution to partition computation across sub-models, and quantising trained weights into compact, low-precision formats.

The proposed implementation targets the GreenWaves Technologies GAP9, which features RISC-V cores alongside a dedicated AI accelerator. We demonstrate that real-time robotic grasp perception is achievable on low-power edge platforms by deploying HGGD-MCU, a hardware-optimised variant of the Heatmap-Guided Grasp Detection (HGGD) architecture [6]. The key contributions of this work are as follows: a) a pipeline methodology to efficiently downscale and run a large 6-Dof grasping model on a low-power MCU such as the GAP9; b) the benchmarking of the proposed method against other state-of-the-art models using average precision (AP), demonstrating competitive performance; c) the evaluation of the model’s inference time when executed on the MCU.

II. BACKGROUND

A. 6D Grasping Perception

6D grasping perception involves the manipulation of objects in six degrees of freedom: three translational (x, y, z) and three rotational (roll, pitch, yaw). Current state-of-the-art techniques use RGBD cameras and point cloud representations to infer grasp configurations straight from raw sensory input [7] [8].

The main challenge in 6D grasping perception is the generalisation from training data to real-world viability [9]. Due to the complexity of dynamic real-world environments, grasping models have to generalise their training data to varying object geometries and material properties, while dealing with inconsistent environments and possibly limited visibility. Consequently, 6D grasping models require substantial high-quality training data and increased computational power for data processing [6] [9].

B. GAP9

GAP9 is a low-power, low-latency processor designed for efficient signal processing across voice, image, and audio

modalities. It is optimised for real-time execution of Neural Network (NN) workloads, achieving high performance with reduced power consumption by leveraging a cluster of highly specialised RISC-V cores capable of executing floating-point multiply-accumulate (FMA) operations. This architecture mirrors the functionality of Neural Processing Units (NPUs) found in modern CPUs and System-on-Chips (SoCs), enabling accelerated tensor computation through hardware-level parallelism.

The SoC operates at an internal clock frequency of up to 370MHz, with Dynamic Voltage and Frequency Scaling. The architecture includes a Fabric Controller (FC) core that orchestrates system-level operations and a cluster of nine additional RISC-V cores, each with identical specifications to the FC. These cores execute independently, allowing concurrent processing of NN layers. A dedicated accelerator core, NE16, further enhances NN inference by offloading convolutional computations.

The FC provides 1.5MB interleaved and 64kB non-interleaved L2 memory, a 2MB non-volatile eMRAM and a 2kB instruction cache. The cluster has access to a 128kB shared data memory, and features a hierarchical instruction cache with 4kB shared memory and 6kB private memory distributed among the cores.

III. METHODS

A. Heatmap-Guided Grasp Detection (HGGD)

For embedded grasping perception, we utilised the HGGD architecture. The architecture generates grasps by encoding grasp heatmaps from RGBD images, which guide the generation process. By processing only relevant image regions, it handles efficiently semantic and geometrical representations [6]. HGGD consists of two separate models: AnchorNet to extract semantic features from the input and generates heatmaps, and LocalNet to generate grasps using a novel semantic-to-point feature extraction.

1) *AnchorNet*: An encoder-decoder model that generates heatmaps for different attributes of the RGBD image. The encoder is based on *ResNet34*, a residual learning network with 34 layers [10]. *ResNet34* extracts features from the preprocessed RGBD image which are subsequently combined with various anchors (possible grasping points) sampled from the original image in the decoder [11]. AnchorNet uses Convolutional Neural Networks (CNNs) to generate anchor-heatmaps for attributes such as width, rotation, and depth, identifying possible grasping regions.

2) *LocalNet*: LocalNet takes as an input a point cloud derived from the original RGBD image and a set of anchors sampled from AnchorNet. It then uses the grasp attributes of each anchor to predict the remaining attributes and create multiple valid 6D grasps.

Heatmap-identified regions likely to contain graspable objects, are mapped to the point cloud to locate the anchors in 3D space. The point cloud is subsequently combined with semantic features from AnchorNet, processed using a custom lightweight PointNet feature extractor, enabling a semantic-to-point feature extraction [12]. These features are used by a

grasp generator to predict the missing attributes and refine the anchors from AnchorNet.

HGGD achieves state-of-the-art performance, with equivalent performance to models like GSNet over the GraspNet-1Billion dataset. It outperforms other models such as TransGrasp and REGNet [13] [14], especially in terms of inference speed, running more than twice as fast as GSNet [15].

B. Optimisation Techniques

This section discusses different optimisation techniques used to enable real-time MCU execution.

1) *Reducing Input Size*: One of the key optimisations for CNNs involves the reduction of the input image size [16]. Since CNNs store weights as kernels, lowering the image resolution can significantly reduce memory usage during convolution operations without impacting the model size. This is particularly important for the GAP9, which has limited L2 memory. By downscaling the input resolution from 640×360 to 320×160 pixels, the input size is reduced by approximately 75%, leading to improved memory usage and reduced latency due to faster transfers between L2 and L3 memory.

2) *Pipeline Execution*: To conserve RAM and flash, the model is partitioned into smaller functionally-equivalent sub-models, each processed sequentially. By utilising multiple MCUs in series, the processing of different sections of the network can be parallelised, with the output from one MCU being used as an input for the next. The model is partitioned into four sub-models, executed in the following order:

- 1) ResNet-MCU (ResNet34 feature extractor / encoder)
- 2) AnchorNet-MCU (heatmap generation / decoder)
- 3) PointNet-MCU (semantic-to-point feature extraction)
- 4) LocalNet-MCU (grasp refinement)

The partitioning into the four sub-models allows a clear and consistent data flow, both computationally and semantically. Additionally, since none of the models are resized in any way, the weights from the original HGGD implementation can be losslessly transferred to the sub-models. The final adapted architecture of AnchorNet and LocalNet can be seen in Figures 2 and 3 respectively.

3) *Quantisation*: Using the GAP9's scaled quantisation method [17], the weights of the model were quantised from float32 to int8, reducing memory usage by a factor of four. While quantisation may impact signal quality, prior studies show minimal practical effects on performance [18].

4) *Targeting Hardware Features*: To maximise inference performance on the GAP9, we leveraged the NE16 NN accelerator and parallel processing capabilities. The NE16 is optimised for the height, width, channels (HWC) layout of input tensors, and the GAP9 clusters are designed for linear or piecewise data access. Efficient data management is critical, as the GAP9 does not incorporate any data caches. We used the Autotiler tool of the GAP9 SDK to optimise data layout and minimise data transfer latency.

IV. EXPERIMENTAL METHODOLOGY

We conducted multiple experiments to evaluate our results, with detailed setup and methodology discussed in this section.

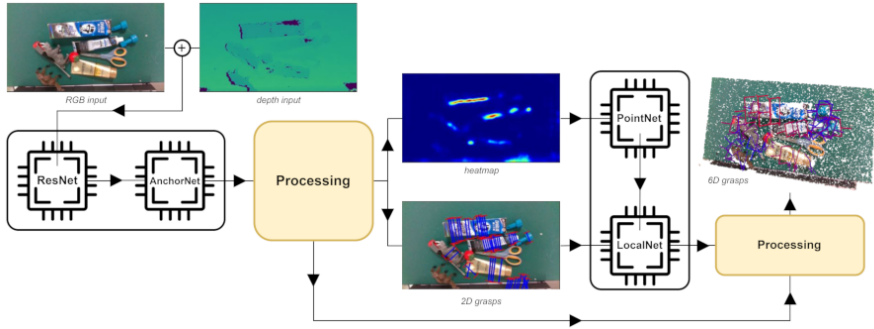


Fig. 1. Edge grasping perception pipeline. The input is passed to a sequence of two MCUs running ResNet-MCU and AnchorNet-MCU. After post processing the output of AnchorNet-MCU, the resulting heatmaps and 2D grasps are used as input for the PointNet-MCU and LocalNet-MCU models running on two additional MCUs. The output of LocalNet-MCU together with additional post processing can be subsequently converted into 6D grasps.



Fig. 2. Adapted architecture of AnchorNet. The dotted line represents the partitioning point, where the original model is split into ResNet-MCU and AnchorNet-MCU.

A. Average Precision

To validate the proposed reduced pipeline, we replicated the original HGGD AP experiments and extended the evaluation by benchmarking against several state-of-the-art methods. The experiments mainly consisted of model evaluation on the testing data of the GraspNet-1Billion dataset [19].

We recorded the AP of the reduced model on the Seen, Similar, and Novel subsets of the testing data, with friction coefficients of $\mu = 1, 0.8, 0.4$. “Seen” data consists of objects present in the training data, “Similar” data includes unseen objects that look similar to ones seen in the training data, and “Novel” data consists of unseen objects that have little to no resemblance to objects seen in the training data.

To maintain consistency with the original HGGD study, we adopted the same set of hyperparameters. For a detailed discussion of their selection process and impact on model performance, the reader is referred to the original paper. The only additional hyperparameter introduced in this work is the input resolution, which was set to 320×160 ; the lowest

Fig. 3. Adapted architecture of LocalNet. The dotted line represents the splitting point of the original model into PointNet-MCU and LocalNet-MCU.

resolution compatible with the original network. At the same time, we incorporated the optimisation techniques discussed in section III-B, allowing for a direct comparison with both the GraspNet-1Billion baseline and the state-of-the-art GSNet.

The test set was executed on the GAP9 simulator GVSOC, and focused on the proposed pipeline execution approach, assessing its feasibility and performance on embedded hardware, without considering the data transfer overhead.

B. Memory requirements

To evaluate the impact of the different optimisation techniques on memory usage, we measured flash, RAM, and L2 memory consumption on the GAP9 platform.

A baseline was established using the partitioned sub-models with no optimisation applied to serve as a reference point. These are referred to as “Original”.

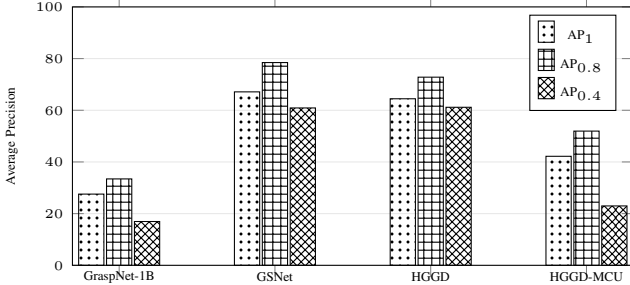


Fig. 4. Measured AP for the “Seen” dataset.

Different optimisation techniques were then applied to the decomposed models. More specifically, the input size of the data was reduced, the models were quantised from float32 to int8, and finally the number of model layers were reduced. The final, optimised models are labeled as “Optimised”.

C. Inference time

Inference time was measured across all four sub-models. Execution times were recorded in processor cycles and later converted to milliseconds using the clock frequency of the MCU, based on the methodology of [20].

Each sub-model was executed 100 times, and the resulting inference times were aggregated to estimate the total forward pass duration. Initial analysis revealed that the distribution of execution times was non-normal, preventing direct calculation of reliable confidence intervals. To address this, we employed bootstrap resampling: 25 samples were randomly drawn with replacement from the measured inference times, repeated 400 times to generate a bootstrapped distribution of the mean. Normality of the bootstrapped means was verified using the Shapiro-Wilk test, which yielded a p-value of 0.265, indicating no significant deviation from normality. This enabled the computation of statistically valid metrics, including t-values and confidence intervals.

V. RESULTS

A. Average Precision

Figures 4, 5 and 6 demonstrate the recorded AP_μ where μ is the friction coefficient for the Seen, Similar, and Novel datasets respectively. To complement these results, Table II provides a broader comparison against state-of-the-art models. “HGGD” refers to the original HGGD implementation, while “HGGD-MCU” represents our reduced pipeline.

B. Memory requirements

Plots 7-9 use a logarithmic scale to highlight significant memory variations across models. The available memory capacity is indicated by the upper bound of the y-axis.

On the GAP9 platform, flash memory usage (Figure 7) is significantly reduced by partitioning the original models into smaller sub-models. All model variants fit well within the available flash capacity, indicating that flash is not a limiting factor in this setup.

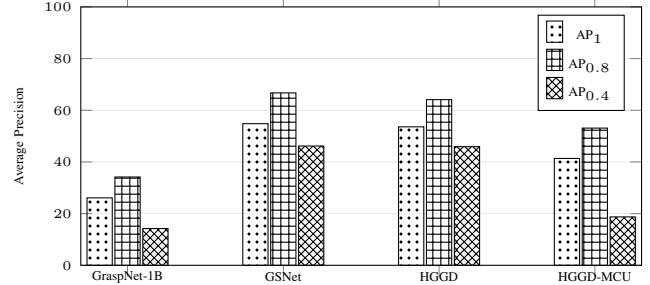


Fig. 5. Measured AP for the “Similar” dataset.

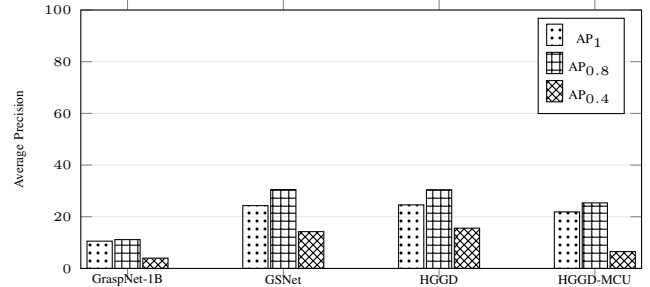


Fig. 6. Measured AP for the “Novel” dataset.

Regarding L2 and RAM requirements (Figures 8 and 9), models exceeding the L2 cache limit are automatically mapped to RAM, ensuring execution remains within the overall memory constraints. Segmenting the original architectures greatly reduces both L2 cache and RAM usage.

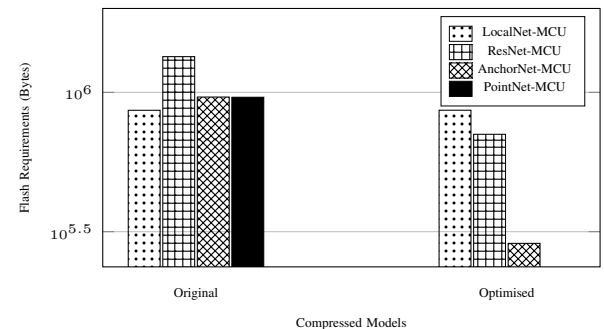


Fig. 7. Flash requirements for the GAP9

C. Measuring inference time

The GAP9 successfully processed the input of the HGGD-MCU model, achieving an average throughput of 740.47 ± 0.0046 milliseconds. Performance analysis revealed that PointNet-MCU was a significant bottleneck, as the original code is hardcoded to operate with a batch size of 1, and modifying this results in errors. As a workaround, we performed 64 passes through the network, which significantly impacted processing speed. Table I presents the inference times for each sub-model when executed on the GAP9.

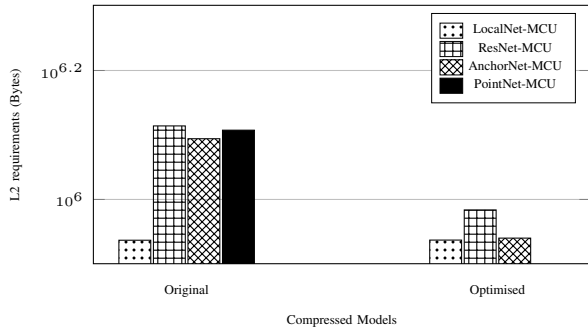


Fig. 8. L2 requirements for the GAP9

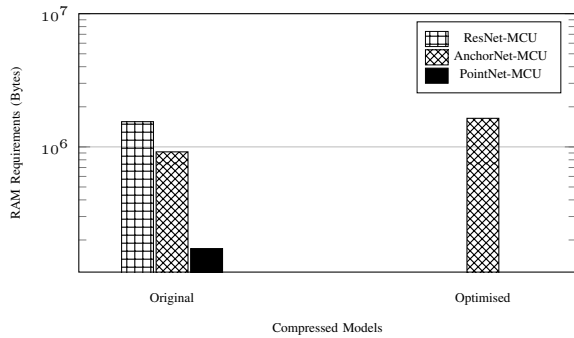


Fig. 9. RAM requirements for the GAP9

VI. DISCUSSION

A. Average Precision

Validation on the GraspNet-1Billion dataset confirmed that our reduced pipeline, HGGD-MCU delivered competitive results. Despite a lower input data resolution, the model performed closely to state-of-the-art approaches, such as GSNet and the original HGGD, when $\mu = 1$ or 0.8, with a noticeable performance drop at $\mu = 0.4$.

As listed in Table II, methods such as [21] and [22] report higher accuracy scores. However, it is important to note prior works were not designed with resource-constrained hardware in mind. In contrast, our work explicitly targets deployment on low-power MCUs. While this makes direct comparison somewhat imbalanced, we include these baselines to position our approach within the broader context of grasp detection. The results highlight the practical trade-offs between model complexity and deployability on edge devices.

B. Memory requirements

The observed flash memory trends align with expectations. Techniques that preserve parameter count, such as lowering the resolution of the input data, maintain similar flash usage. In contrast, quantisation and model segmentation significantly reduce the number of parameters, leading to a substantial reduction in flash utilisation.

RAM usage is primarily driven by intermediate activations during inference. Reducing network depth does not necessarily

Model	Inference time (ms)
ResNet-MCU	15.13
AnchorNet-MCU	44.96
PointNet-MCU	674.79
LocalNet-MCU	5.58

TABLE I
INFERENCE TIME FOR EACH MODEL IN MILLISECONDS

lower RAM demands, especially when memory usage is dominated by feature maps. However, techniques like resolution reduction and quantisation directly reduced feature map size or precision, thereby reducing RAM consumption. Model partitioning also reduces peak memory usage, since each sub-model is executed independently.

Hierarchical memory architectures further improve efficiency. When sub-models exceed the on-chip L2 cache, they spill into system RAM, ensuring that they remain fully operable. At the same time, smaller models that fully fit within L2 benefit from lower latency due to faster memory access. These findings confirm that careful selection and tuning of optimisation strategies are critical for efficient memory use on resource-constrained platforms such as the GAP9.

C. Inference time

Among the validated models, PointNet-MCU was the most computationally expensive, accounting for approximately 90% of the total inference time. This cost is attributed to the hard-coded batch size of 1, as NNTool failed when attempting to set a batch size of 64. Future updates to the tool may address this issue, while alternative workarounds could be explored.

With an inference time of 740ms, the model demonstrates speeds that can be considered adequate for many grasping tasks, particularly in scenarios where robotic arms operate at slower speeds. For instance, in tasks involving delicate handling or precise placements, the robot's movement often dictates the overall operation speed rather than the computational latency. Further optimisations, such as reducing the computational overhead of PointNet or parallelising certain operations, could reduce inference times even further, making the system more versatile and suitable for real-time applications. This study underscores the potential of the GAP9 as a reliable and efficient platform for edge AI tasks in robotics.

D. Exploration

We applied a range of optimisation techniques to reduce both inference time and memory usage. Despite these efforts, certain layers proved incompatible with the deployment toolkit, and some model variants exceeded the GAP9's memory capacity or relied on unsupported operations.

To address near real-time performance requirements, we partitioned the grasp perception pipeline into four sub-models, each responsible for a specific stage of the original architecture. This approach allowed a pipelined inference but introduced overhead due to the transfer of intermediate results between stages. In principle, this latency could be mitigated through the deployment of multiple GAP9s in parallel, each running a pipeline stage. Our findings suggest that model

Method	Seen			Similar			Novel		
	AP ₁	AP _{0.8}	AP _{0.4}	AP ₁	AP _{0.8}	AP _{0.4}	AP ₁	AP _{0.8}	AP _{0.4}
[6]	64.45	72.81	61.16	53.59	64.12	45.91	24.59	30.46	15.58
[15]	67.12	78.46	60.9	54.81	66.72	46.17	24.31	30.52	14.23
[21]	68.21	79.6	63.54	61.19	73.60	53.77	25.48	31.46	13.85
[22]	74.33	85.77	63.89	64.36	76.76	55.25	27.56	34.09	20.23
This work	42.19	51.94	22.98	41.36	53.1	18.73	21.87	25.37	6.51

TABLE II
AP COMPARISON WITH STATE-OF-THE-ART MODELS

decomposition and offloading to a host processor or multiple MCUs is a promising direction for increasing throughput.

VII. CONCLUSIONS

This study explored the feasibility of deploying a state-of-the-art robotic grasping perception model on resource-constrained MCUs. Our work focused on optimising the HGGD model for 6D grasping tasks on the GAP9 SoC.

We demonstrated that by reducing the input size and partitioning the model we achieved a strong performance on the GraspNet-1Billion dataset.

Reducing the input resolution lowered significantly the model's memory requirements with only a modest impact on performance. Model partitioning further reduced both flash and memory usage at no additional performance cost. However, this came at the cost of increased inference time, as models have to be loaded and unloaded from the MCU as the model progresses. This limitation could be mitigated by parallelising execution across multiple MCUs. Additionally, quantisation reduced significantly flash and memory footprints.

Future work will focus on extending these findings to a broader range of MCUs and evaluate system performance in robotic hardware setups. We also encourage further investigation into structural optimisations, such as layer pruning, which may yield additional gains at the cost of retraining. These directions will help advance the deployment of complex vision-based robotic systems on low-power, embedded hardware.

REFERENCES

- [1] Kevin Tai, Abdul-Rahman El-Sayed, Mohammadali Shahriari, Mohammad Biglarbegian, and Shohel Mahmud. State of the art robotic grippers and applications. *Robotics*, 5(2):11, 2016.
- [2] S. Ekvall and D. Kragic. Interactive grasp learning based on human demonstration. In *IEEE International Conference on Robotics and Automation, 2004. Proceedings. ICRA '04. 2004*, volume 4, pages 3519–3524 Vol.4, 2004.
- [3] Charalampos S. Kouzinopoulos, Eleftheria Maria Pechlivanli, Nikolaos Giakoumoglou, Alexios Papaioannou, Sotirios Pemas, Panagiotis Christakakis, Dimosthenis Ioannidis, and Dimitrios Tzovaras. A citizen science tool based on an energy autonomous embedded system with environmental sensors and hyperspectral imaging. *Journal of Low Power Electronics and Applications*, 14(2), 2024.
- [4] Susanne Brockmann and Tim Schlippe. Optimizing convolutional neural networks for image classification on resource-constrained microcontroller units. *Computers*, 13(7):173, 2024.
- [5] Alexios Papaioannou, Charalampos S Kouzinopoulos, Dimosthenis Ioannidis, and Dimitrios Tzovaras. An ultra-low-power embedded ai fire detection and crowd counting system for indoor areas. *ACM Transactions on Embedded Computing Systems*, 22(4):1–20, 2023.
- [6] Siang Chen, Wei Tang, Pengwei Xie, Wenming Yang, and Guijin Wang. Efficient heatmap-guided 6-dof grasp detection in cluttered scenes. *IEEE Robotics and Automation Letters*, 2023.
- [7] Shubham Agrawal, Nikhil Chavan-Dafle, Isaac Kasahara, Selim Engin, Jinwook Huh, and Volkan Isler. Real-time simultaneous multi-object 3d shape reconstruction, 6dof pose estimation and dense grasp prediction. In *2023 IEEE/RSJ International Conference on Intelligent Robots and Systems (IROS)*, pages 3184–3191. IEEE, 2023.
- [8] Pengwei Xie, Siang Chen, Wei Tang, Dingchang Hu, Wenming Yang, and Guijin Wang. Rethinking 6-dof grasp detection: A flexible framework for high-quality grasping. *arXiv preprint arXiv:2403.15054*, 2024.
- [9] Dominik Bauer, Peter Hönig, Jean-Baptiste Weibel, José García-Rodríguez, Markus Vincze, et al. Challenges for monocular 6d object pose estimation in robotics. *IEEE Transactions on Robotics*, 2024.
- [10] Kaiming He, Xiangyu Zhang, Shaoqing Ren, and Jian Sun. Deep residual learning for image recognition. In *Proceedings of the IEEE conference on computer vision and pattern recognition*, pages 770–778, 2016.
- [11] Xinwen Zhou, Xuguang Lan, Hanbo Zhang, Zhiqiang Tian, Yang Zhang, and Narming Zheng. Fully convolutional grasp detection network with oriented anchor box. In *2018 IEEE/RSJ International Conference on Intelligent Robots and Systems (IROS)*, pages 7223–7230. IEEE, 2018.
- [12] Charles R Qi, Hao Su, Kaichun Mo, and Leonidas J Guibas. Pointnet: Deep learning on point sets for 3d classification and segmentation. In *Proceedings of the IEEE conference on computer vision and pattern recognition*, pages 652–660, 2017.
- [13] Zhixuan Liu, Zibo Chen, Shangjin Xie, and Wei-Shi Zheng. Transgrasp: A multi-scale hierarchical point transformer for 7-dof grasp detection. In *2022 International Conference on Robotics and Automation (ICRA)*, pages 1533–1539. IEEE, 2022.
- [14] Binglei Zhao, Hanbo Zhang, Xuguang Lan, Haoyu Wang, Zhiqiang Tian, and Nanning Zheng. Regnet: Region-based grasp network for end-to-end grasp detection in point clouds. In *2021 IEEE international conference on robotics and automation (ICRA)*, pages 13474–13480. IEEE, 2021.
- [15] Chenxi Wang, Hao-Shu Fang, Minghao Gou, Hongjie Fang, Jin Gao, and Cewu Lu. Graspness discovery in clutter for fast and accurate grasp detection. In *Proceedings of the IEEE/CVF International Conference on Computer Vision*, pages 15964–15973, 2021.
- [16] Stefan Wermter, Mats L. Richter, Wolf Bytner, Ulf Krumnack, Anna Wiedenroth, Ludwig Schallner, and Justin Shenk. *(Input) Size Matters for CNN Classifiers*. Artificial Neural Networks and Machine Learning ICANN 2021. Springer, 2021.
- [17] Steve Dai, Rangha Venkatesan, Mark Ren, Brian Zimmer, William Dally, and Brucek Khailany. Vs-quant: Per-vector scaled quantization for accurate low-precision neural network inference. *Proceedings of Machine Learning and Systems*, 3:873–884, 2021.
- [18] Soheil Hashemi, Nicholas Anthony, Hokchhay Tann, R Iris Bahar, and Sherief Reda. Understanding the impact of precision quantization on the accuracy and energy of neural networks. In *Design, Automation & Test in Europe Conference & Exhibition (DATE)*, 2017, pages 1474–1479. IEEE, 2017.
- [19] Hao-Shu Fang, Chenxi Wang, Minghao Gou, and Cewu Lu. Graspnet-1billion: A large-scale benchmark for general object grasping. In *Proceedings of the IEEE/CVF conference on computer vision and pattern recognition*, pages 11444–11453, 2020.
- [20] Alexandru Buturugă, Rodica Claudia Constantinescu, and Dan Alexandra Stoicescu. Time measurement techniques for microcontroller performance analysis. In *23rd International Symposium for Design and Technology in Electronic Packaging*, pages 38–43. IEEE, 2017.
- [21] Xiao-Ming Wu, Jia-Feng Cai, Jian-Jian Jiang, Dian Zheng, Yi-Lin Wei, and Wei-Shi Zheng. An economic framework for 6-dof grasp detection, 2024.
- [22] Hanwen Wang, Ying Zhang, Yunlong Wang, and Jian Li. 6-dof grasp detection in clutter with enhanced receptive field and graspable balance sampling, 2024.